ELSEVIER

15 May 1995

PHYSICA C

Physica C 247 (1995) 297–308

Strong damping of the c-axis plasmon in high-T_c cuprate superconductors

Jae H. Kim [a], H.S. Somal [a], M.T. Czyzyk [a], D. van der Marel [a] A. Wittlin [b], A.M. Gerrits [b] V.H.M. Duijn [c], N.T. Hien [c] A.A. Menovsky [c]

[a] *Laboratory of Solid State Physics, Materials Science Center, University of Groningen, Nijenborgh 4, 9747 AG Groningen, The Netherlands*
[b] *High Field Magnet Laboratory, University of Nijmegen, Toernooiveld 1, 6525 ED Nijmegen, The Netherlands*
[c] *van der Waals-Zeeman Laboratory, University of Amsterdam, Valckenierstraat 65, 1018 XE Amsterdam, The Netherlands*

Received 17 February 1995; revised manuscript received 30 March 1995

Abstract

We analyze the infrared reflectivity of $La_{1.85}Sr_{0.15}CuO_4$ single crystals with E parallel to the c-axis. The plasma edge at around 6 meV (50 cm^{-1}), which occurs only for $T < T_c$, is due to Cooper-pair tunneling. This low value of the plasma edge is shown to be consistent with the c-axis plasma frequency obtained from LDA band structure calculations (> 0.1 eV) if we take into account that the single-particle charge transport along the c-axis is strongly incoherent in the normal state, and remains so in the superconducting state. From a comparison of the optical conductivity with model calculations based on s- and d-wave weak-coupling theory in the dirty limit, we find no evidence for a reduction of the c-axis quasi-particle scattering rate below T_c. The c-axis scattering rate, the normal-state c-axis plasma frequency, and T_c obey $h\gamma > h\nu_p \gg 3.5k_BT_c$, which is exactly opposite to the clean limit.

1. Introduction

One of the peculiar aspects of the high-T_c cuprate superconductors is the large anisotropy of their physical properties, related to their layered crystal structure. Although the anisotropy, following from a conventional Fermi-liquid approach based on LDA (local density approximation) band structure calculations, is of the order of 10 in most of these compounds, experimentally it is found to be much larger, as follows from e.g. the optical response and the normal-state resistivity. One can also compare the theoretical and experimental values of the *ab*-plane and the c-axis plasma frequencies in order to check further the reliability of LDA-based band structure calculations.

In the superconducting state the anisotropy manifests itself strongly in the penetration depth measurements and in the far-infrared spectra. Although the normal state c-axis response looks insulator-like, in the superconducting state in some materials a plasmon-related zero crossing of the real part of the dielectric function (ϵ') is found, but again at an energy two orders of magnitude below the value expected from LDA band structure calculations. Soon after the discovery of high-T_c superconductivity, a reflectivity edge in the spectra of polycrystalline $La_{1.85}Sr_{0.15}CuO_4$ was observed below T_c near 50 cm^{-1} and it was eventually attributed to a plasmon along the c-axis [1–5]. Subsequently, Sherwin et al. [6] proposed that this low plasma frequency and its temperature dependence could be explained by a strong damping of the c-axis plasmon or the opening of a gap below T_c. However,

SSDI 0921-4534(94)00198-0

due to ambiguities in the interpretation of the optical data of the strongly anisotropic polycrystalline material, no firm conclusions were then reached regarding this point.

More recent results obtained for single crystals of $La_{1.85}Sr_{0.15}CuO_4$[7], $Bi_2Sr_2CaCu_2O_8$ [8], $YBa_2Cu_3O_7$[9,10], and $YBa_2Cu_4O_8$ [11] show that such anisotropy of low-frequency optical properties and the very low value of the *c*-axis plasmon are indeed a common feature of the high-T_c cuprate superconductors, and raise the question as to their origin.

In a number of recent papers [7,12] a large effective mass along the *c* direction has been assumed to explain the far-infrared spectra and the penetration depth of single crystals of $La_{2-x}Sr_xCuO_4$. A mass enhancement could follow from e.g. spin-charge separation [13–17]. Alternatively, in the context of a Fermi-liquid description, incoherent *c*-axis transport arising from elastic and inelastic scattering processes has been proposed by, respectively, Graf et al. [18] and Rojo et al. [19]. Such scenarios could lead to incoherent transport at energies larger than typically $\tilde{t}_\perp/8$ [20] where $\tilde{t}_\perp$ is the effective interlayer hopping energy. Such approaches are still within the general paradigm of Fermi liquid theory in contrast to other approaches based on the concept of spin-charge separation. The Fermi-liquid approaches to this problem have been criticized by Anderson e.g. in Ref. [16].

In this paper we conclude from a quantitative analysis that, for the *c*-axis response of $La_{2-x}Sr_xCuO_4$, the absence of a plasma pole above T_c and the strong reduction of the plasma frequency below T_c indeed result from *a strong quasi-particle damping along the c-axis*, both in the normal and in the superconducting states.

2. Experiment

2.1. Sample preparation

Single crystals of $La_{2-x}Sr_xCuO_4$ with nominal Sr content of 15% were grown by the traveling-solvent floating-zone method [21]. Electron-probe micro-analysis showed the correct phase with no contamination or inclusion of second phases, and a homogeneous distribution of Sr. The crystals have sharp superconducting transitions with the onset at 35 K at optimal doping and with 90% of the transition within 3 K as determined from AC susceptibility measurements at 3 Gauss and 90 Hz.

Neutron diffraction measurements demonstrated that the as-grown boules contain large single crystalline grains. Samples for reflectivity measurements were cut perpendicular to the *b*-axis and were mechanically polished to optical quality. The surface in the *ac* plane was approximately 4 mm×7 mm. X-ray Laue backscattering showed a correct orientation with sharp, well-defined single diffraction spots.

2.2. Reflectivity measurements

Polarized infrared reflectivity spectra were measured in two different laboratories between 10 and 10000 cm^{-1} at temperatures between 8 and 300 K using rapid-scan Fourier-transform infrared (FTIR) spectrometers equipped with a continuous-flow liquid-He cryostat. The data obtained in the two laboratories on crystals of the same nominal composition are in good agreement with each other, and with those of Tamasaku et al. [7].

3. Results

3.1. Normal-state reflectivity

In Fig. 1 we display the reflectivity (R) of a $La_{1.85}Sr_{0.15}CuO_4$ single crystal with $\boldsymbol{E} \parallel \boldsymbol{c}$ at various temperatures. An expanded view of the low-frequency region is given in Fig. 2. The normal-state reflectivity is replotted in Fig. 3 (circles) for closer inspection. It is quite characteristic of an ionic insulator with strong infrared-active phonons dominating the far-infrared region. At low frequencies there is a Hagen-Rubens type of upturn, indicative of a poor conductor: $R(\nu) = 1 - 2\sqrt{\nu/\sigma_0}$ where σ_0 is the DC conductivity. The real part of the conductivity (Re σ) is nearly constant in the relevant frequency range ($\approx 7\ \Omega^{-1}cm^{-1}$).

As we have no á priori knowledge about the frequency dependence of the electronic contribution to the conductivity, we attempted to fit the experimental data assuming that the real part of the conductivity has the Drude–Lorentz line shape Re $\sigma(\nu) = \sigma_0(1+\nu^2/\gamma^2)^{-1}$ where γ is the damping rate. As we will see later, Re $\sigma(\nu)$ turns out to be a very broad

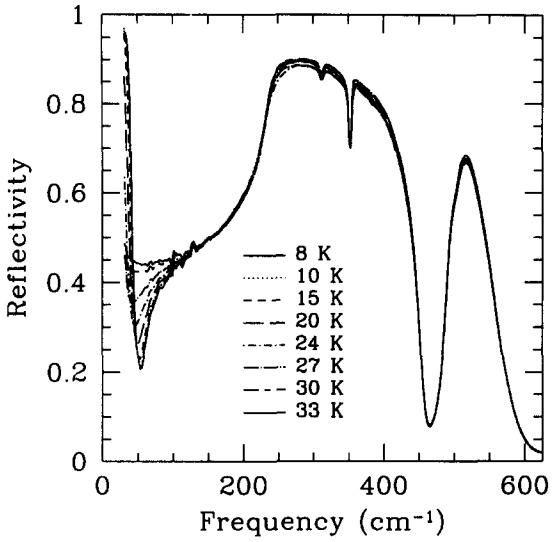

Fig. 1. The c-axis reflectivity of $La_{1.85}Sr_{0.15}CuO_4$ at 8, 10, 15, 20, 24, 27, 30 and 33 K.

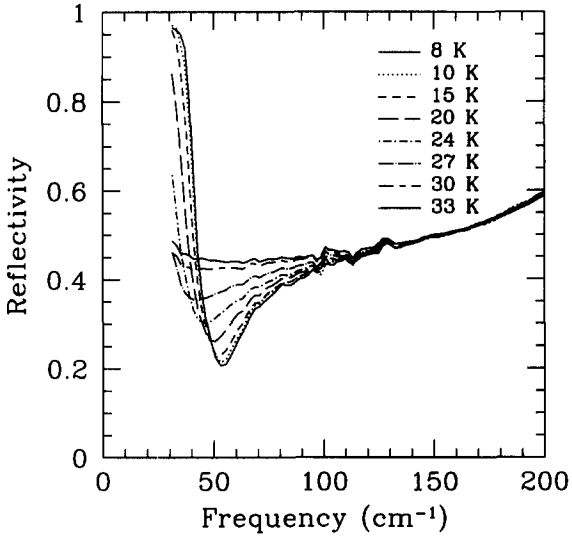

Fig. 2. The low-frequency c-axis reflectivity of $La_{1.85}Sr_{0.15}CuO_4$ at 8, 10, 15, 20, 24, 27, 30 and 33 K.

and featureless function, and with this formula we are effectively testing the value of Re σ at $\nu = 0$, and its departure thereof in leading orders of ν^2.

Assuming therefore for the moment that we may write Re $\sigma(\nu) = \sigma_0(1+\nu^2/\gamma^2)^{-1}$, and by fitting σ_0, γ, and the center frequency, oscillator strength, and damping rate of two strong (ω_i = 242, 494 cm^{-1}) and two weak (ω_i = 312, 351 cm^{-1}) transverse optical (TO) phonons, we obtained the fit displayed in Fig. 3 (solid curve). A successful fit in the range of 20 to 650 cm^{-1} is obtained only if we assume that $\gamma > 4500$ cm^{-1} in the above formula. To demonstrate the effect of assuming a smaller value for γ we also display in Fig. 3 a curve corresponding to γ = 292 cm^{-1} with all the other parameters the same as before. Clearly there are now significant deviations in the frequency range between 200 and 800 cm^{-1}. We made similar observations on another sample from the same batch of single crystals. This is also born out by our analysis of the spectra at temperatures above and below T_c, and from re-analyzing the experimental data published by Tamasaku et al. [7] (see also Fig. 4, and the corresponding discussion in Section 3.2).

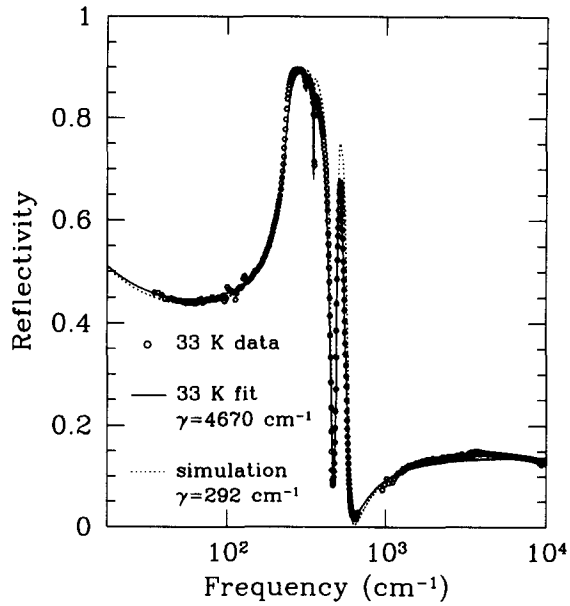

Fig. 3. The c-axis reflectivity of $La_{1.85}Sr_{0.15}CuO_4$ at 33 K (circles) along with the least-square-fitted curve (solid line). The best fitting parameters are $\epsilon_\infty = 4.75$, $\sigma_0 = 7\ \Omega^{-1}$ cm^{-1}, $\gamma = 4670$ cm^{-1}, and $\nu_p = 1320$ cm^{-1}. The TO phonons were parameterized with $\{\omega_i$ (cm^{-1}), γ_i (cm^{-1}), $S_i\}$ $(i = 1 \cdots 4)$: {241.5, 24.8, 17.6}, {312.0, 3.0, 0.019}, {351.0, 3.0, 0.044}, {494.1, 12.8, 0.33}. In order to test the reliability of the fit, we also plot a simulated reflectivity curve (dash-dot line) corresponding to $\gamma = 292$ cm^{-1} and $\nu_p = 330$ cm^{-1} with the phonon parameters of the best fit. Although the change in γ and ν_p will not affect the DC conductivity, the overall agreement with experiment becomes quite poor. The electronic component of conductivity is indeed quite flat.

A second important observation from looking at Fig. 3 is that there is no noticeable influence of the value of

Re σ on the reflectivity spectrum for $\nu > 1000\ \mathrm{cm}^{-1}$: The theoretical spectra for $\gamma \approx 4700\ \mathrm{cm}^{-1}$ and $\gamma \approx 290\ \mathrm{cm}^{-1}$ coincide within the plotting accuracy. Vice versa this implies that for photon energies larger than 0.1 eV the reflectivity is rather insensitive to the detailed behavior of the conductivity and at present we are not able to argue against or in favor of the $\omega^{-1/4}$ scaling law predicted by Clarke, Strong and Anderson [16], hopping-type of behavior, or simple Drude behavior.

On the other hand, none of these models, or in fact any reasonable theory, predicts an abrupt step in σ at frequencies larger than 0.1 eV. We exploit this fact to place an upper bound on the optical effective mass along the c direction by employing the f-sum rule ($\int_0^\infty \mathrm{Re}\ \sigma(\nu)d\nu = ne^2/4m$) where n is the electron density, e the electronic charge, and m the electronic mass. By restricting the integration interval within the bounds of the bandwidth W, while staying below the first interband transitions, $1/m$ would in a single particle picture correspond to Fermi-surface average over the c-axis effective mass tensor element. This implies that $\int_0^W \mathrm{Re}\ \sigma(\nu) = (\pi/4)\nu_p^2$ where ν_p is the plasma frequency in the c direction as would follow from an LDA band structure calculation. By integrating the corresponding expression for Re $\sigma(\nu)$, we can put a lower bound on the plasma frequency $\nu_p = 0.15$ eV (note $\nu_p = \sqrt{2\sigma_0\gamma}$ in the Drude model).

Due to the broadening of Re σ over a large frequency range, the energy ν_p no longer corresponds to the collective mode of the electron gas, i.e., the zero crossing of the real part of the dielectric function (ϵ'). In fact with these parameters the zero crossing of $\epsilon'(\nu) = \tilde{\epsilon}_\infty - \nu_p^2/(\nu^2 + \gamma^2)$ (where $\tilde{\epsilon}_\infty$ is the high-frequency dielectric constant prevailing in the far-infrared spectral region) occurs for $\nu^2 < 0$, and the plasmon has a diffusive pole in the normal state. Hence, the c-axis plasmon is overdamped in the normal state (rather than extremely small in energy or completely absent) due to the broadening of Re σ, and the c-axis plasma frequency is of the same order of magnitude as that predicted by LDA band structure calculations. We return to microscopic physical models for this broadening in Section 4 of this paper.

3.2. Superconducting-state reflectivity

As the temperature goes below T_c, we observe a remarkable development of a plasma edge, which moves to higher frequencies with decreasing temperature and reaches about $2k_BT_c$ ($50\ \mathrm{cm}^{-1}$ or 6 meV) as $T \to 0$. At the same time, we notice that the changes in reflectivity for $\nu > 200\ \mathrm{cm}^{-1}$ are quite small. The phonon at 241.5 cm^{-1} has a very large oscillator strength, which masks the electronic contribution to the conductivity in this range. However, we notice that the minima at $460\ \mathrm{cm}^{-1}$ and $630\ \mathrm{cm}^{-1}$, and the maximum at $510\ \mathrm{cm}^{-1}$ have only very weak temperature dependence. This implies that the electronic contribution to the conductivity σ at frequencies higher than approximately $4k_BT_c$ is not affected by the superconducting phase transition. In this respect the present behavior is not much different from what happens in a classical BCS superconductor.

Following the procedure outlined in one of our earlier publications about the *ab*-plane response of $YBa_2Cu_3O_{7-\delta}$ [22], for frequencies not too small compared to the scale of gap energy the reflectivity in the superconducting state can be analyzed in a phenomenological way using the two-fluid Gorter–Casimir model for the dielectric function ϵ:

$$\epsilon(\nu) = \tilde{\epsilon}_\infty \left(1 - \frac{\tilde{\nu}_\phi^2}{\nu^2}\right) + \frac{2i\sigma_n(T)}{\nu(1 - i\nu/\gamma)}, \qquad (1)$$

where $\tilde{\nu}_\phi$ is the phason frequency and $\sigma_n(T)$ is the conductivity of the normal fluid. In a more conventional notation $c\tilde{\epsilon}_\infty^{-1/2}\tilde{\nu}_\phi^{-1}$, (where c is the speed of light) is just the penetration depth in the superconducting state. However, because in the present case there is no plasmon mode associated with the charge carriers in the normal state, $\tilde{\nu}_\phi$ now corresponds to a collective mode of the superconducting condensate. Due to phase-density conjugation in a superfluid, this can be identified as a collective oscillation of the phase of the order parameter (or 'phason' [23]).

The second term represents the 'normal fluid'. Even in a conventional s-wave superconductor the conductivity is finite (except for $T = 0$) for frequencies below the gap due to the presence of a finite density of quasiparticles which are thermally excited across the gap. If the order parameter has nodes, this effect becomes even bigger. A difficulty arises in employing Eq. (1)

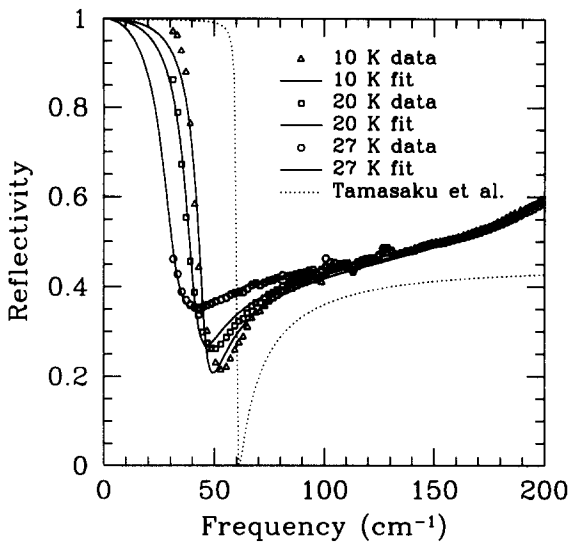

Fig. 4. The low-frequency c-axis reflectivity of $La_{1.85}Sr_{0.15}CuO_4$ at 10, 20 and 27 K along with the fitted curves at each temperature. The fitted curve of Tamasaku et al. for their 8 K data is also shown in dotted line.

at low frequencies (typically smaller than $0.5k_BT_c$) where coherence factors play an important role. As a result the conductivity line-shape becomes manifestly non-Drude like at low frequencies. In the present case we will fit the superconducting-state reflectivity data for frequencies at around $2k_BT_c$ up to 100 cm^{-1}. An important point to be noticed here is that by restricting the fitting range to the region around the plasma minimum, the value for σ_0 is mainly determined by the value of the reflectivity at the minimum, where

$$R = \frac{\sqrt{2} - (1 + \sqrt{1 - \epsilon^{1/2}})^{1/2}}{\sqrt{2} + (1 + \sqrt{1 - \epsilon^{1/2}})^{1/2}}$$

so that $\sigma_n(T)$ can be already read directly from the reflectivity curves using $\sigma_n(T) \approx 2\nu\sqrt{R}$.

The fitting results are summarized in Fig. 4. The dotted curve in Fig. 4 corresponds to the fit parameters used by Tamasaku et al. for 8 K [7]. Note that with their fit parameters ($\tilde{\epsilon}_\infty = 25$, $\tilde{\nu}_\phi = 56$ cm^{-1}, $\tilde{\nu}_p = 60$ cm^{-1}, and $\gamma = 2$ cm^{-1} in the notation of Eq. (2)), nearly all oscillator strength under the conductivity σ collapses into the δ-function at the zero frequency. This essentially corresponds to the clean limit. But, clearly, their fit parameters cannot reproduce the experimental results to a satisfactory extent (Fig. 4). We have obtained a much better fit by assuming again a broad and featureless electronic part of the conductivity σ, as in the normal-state case. Initially we attempted varying all parameters. At all temperatures the best fits indicated that $\nu \ll \gamma$, and only small and unsystematic changes of $\tilde{\epsilon}_\infty$ with temperature were obtained. Therefore we repeated the analysis with $\gamma \to \infty$, replacing $\tilde{\epsilon}_\infty$ by the sum of ϵ_∞ and the oscillator strengths of the four TO phonons (Fig. 1). To estimate the influence of dispersion of the TO phonons, we also did this analysis using the full set of phonon parameters as given in Fig. 1. In either case, it was possible to fit the reflectivity spectra at all temperatures without assuming drastic temperature dependence in the damping rate γ.

The temperature dependence of the reflectivity then follows mainly from those of $\tilde{\nu}_\phi$ and σ_n. The temperature dependence of the two parameters $((\tilde{\nu}_\phi(T)/\tilde{\nu}_\phi(0))^2$ (proportional to the superfluid fraction) and $\sigma_n(T)/\sigma_n(T_c)$, with $\tilde{\nu}_\phi(0) = 38$ cm^{-1} and $\sigma_n(31\text{ K}) = 6.7$ $\Omega^{-1}cm^{-1}$, will be discussed in Section 4 (Fig. 9).

3.3. Kramers–Kronig analysis

Based on our fitting results for the reflectivity spectra, the low-frequency extrapolations for the reflectivity were made with the two-fluid model as explained in the previous section. The low-frequency behavior of $1 - R$ changes from ν^2 in the superconducting state to the Hagen-Rubens behavior $\sqrt{\nu}$ in the normal state. Hence we employed the following dielectric function for extrapolation:

$$\epsilon(\nu) = \tilde{\epsilon}_\infty \left[1 - \frac{\tilde{\nu}_\phi^2}{\nu(\nu + i0^+)} - \frac{\tilde{\nu}_p^2 - \tilde{\nu}_\phi^2}{\nu(\nu + i\gamma)} \right], \quad (2)$$

where $\tilde{\nu}_p$ is the screened plasma frequency in the normal state. In Fig. 5 we present the conductivity of $La_{1.85}Sr_{0.15}CuO_4$ at various temperatures derived from the subsequent Kramers–Kronig analysis. The large value of γ in comparison with the pair-breaking energy scale $3.5k_BT_c$ implies that the c-axis infrared response of $La_{1.85}Sr_{0.15}CuO_4$ belongs to the dirty limit. However, from the conductivity spectra it is quite difficult to identify a clear BCS-like gap. It may be that the order parameter in high-T_c superconductors exhibit d-wave symmetry, in which case one expects much more gradual and smeared frequency dependence in

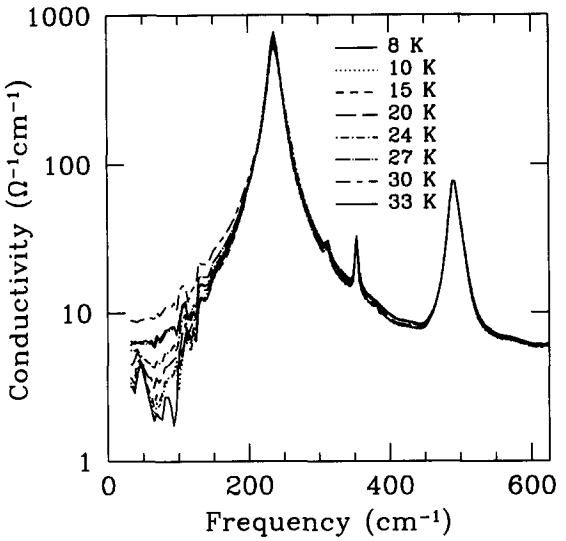

Fig. 5. The c-axis conductivity of $La_{1.85}Sr_{0.15}CuO_4$ at 8, 10, 15, 20, 24, 27, 30 and 33 K.

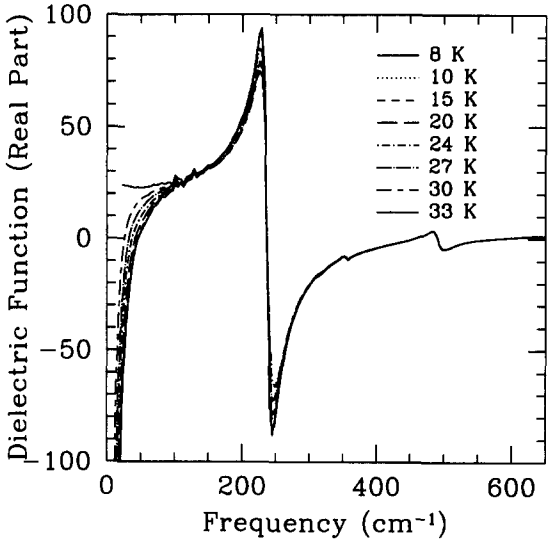

Fig. 6. The real part of the c-axis dielectric function of $La_{1.85}Sr_{0.15}CuO_4$ at 8, 10, 15, 20, 24, 27, 30 and 33 K.

the conductivity. But, even if the BCS theory is valid for $La_{1.85}Sr_{0.15}CuO_4$ and even if the material belongs to the dirty limit, the gap will be very difficult to identify partly because the nearby giant phonon oscillator extends to the expected gap energy, and also because the electronic contribution to the conductivity itself is rather small, which leads to a small *change* in the conductivity. This means whatever spectral feature that may appear due to opening of the gap will be masked and quite weak.

In Figs. 6 and 7 we display the real part of the dielectric function and the loss function of $La_{1.85}Sr_{0.15}CuO_4$, respectively, for various temperatures. Notice that the real part of the dielectric function ϵ' does not have a zero crossing above T_c (overdamped plasmon in the normal state) but as soon as we go below T_c, a zero crossing occurs and it moves to higher energy with decreasing temperature (Fig. 6). The presence of the phason excitation is quite apparent in the loss function, the peaks of which correspond to the longitudinal excitation (Fig. 7).

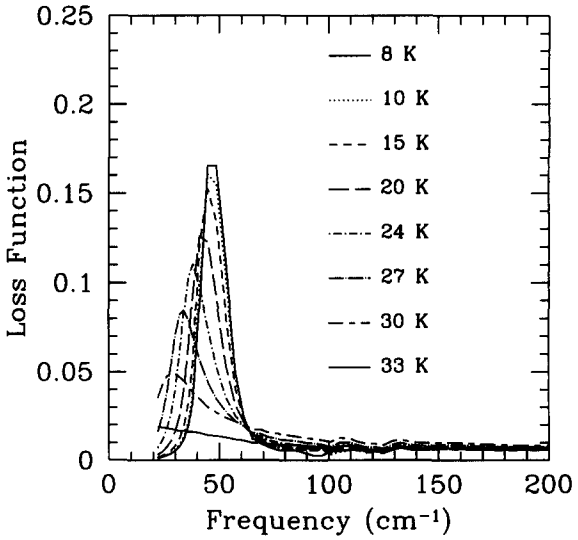

Fig. 7. The c-axis loss function of $La_{1.85}Sr_{0.15}CuO_4$ at 8, 10, 15, 20, 24, 27, 30 and 33 K.

4. Discussion

4.1. The c-axis plasma frequency

In the previous sections we observed that the c-axis plasma frequency (ν_p), defined as $((4/\pi) \times \int_0^W \mathrm{Re}\,\sigma(\nu)d\nu)^{1/2}$ with W a suitably chosen cut-off frequency, is *at least* 0.15 eV. Although the

energy-momentum dispersion obtained from LDA band structure calculations do not correspond quantitatively (or in the present case not even qualitatively) to the single-particle excitation spectra, the value of the single-electron interlayer hopping matrix elements following from such a calculation is, as a rule, quite accurate (because it is a ground-state property). We therefore feel justified in assuming that the lower limit of 0.15 eV for ν_p using the f-sum rule is a measure of the plasma frequency as would follow from a band structure calculation where many-body effects are ignored. As the integration should end below the onset of interband transitions, but at an energy above the highest frequency of the intraband conductivity, an appropriate cut-off frequency W in the integration may not always be available.

To check the above result we calculated the plasma frequency as a function of momentum within the random phase approximation (RPA), using the $E(\boldsymbol{k})$ dispersion of La_2CuO_4 calculated within the self-consistent augmented-spherical-wave (ASW) approximation [24]. The Fermi-surface following from our LDA band structure calculation is roughly a rectangular tube, oriented along the c direction, with the corners of the rectangle near the $(\pi, 0)$ saddle points. There is a clear corrugation of the tube in the c direction. Without such a corrugation the Fermi surface would be ideally two-dimensional, and the material would resemble a layered electron gas with a plasma dispersion obeying $\omega_p(\boldsymbol{k}) = \omega_{p\|}k_\|/\sqrt{k_\|^2 + k_\perp^2}$ for $|\boldsymbol{k}| \to 0$ [25,26] where $\omega_{p\|}$ is the in-plane plasma frequency and $k_\|$ and $k_\perp$ are, respectively, the in-plane and out-of-plane momenta. Note that in this case $\omega_{p\|}/\omega_{p\perp} \to \infty$. On the other hand, from our LDA/RPA calculation we obtained a bare ab-plane plasma frequency of about 4 eV, and a bare c-axis plasma frequency of 0.7 eV. After correcting for the 'background' these correspond to 2 eV for the ab-plane plasmon (well above the onset of the interband electron-hole continuum at 0.5 eV), and 0.35 eV for the c-axis plasmon (below the interband electron-hole continuum). One then expects that the ab-plane plasmon is Landau-damped while the c-axis plasmon is not.

It is an important result that experimentally the situation vis á vis Landau damping is reversed. In the ab-plane dielectric function a clear, though strongly damped, plasma pole is observed near 1 eV [27], whereas the c-axis plasmon is completely overdamped in the normal state. If the plasma frequency in the ab plane is calculated using the f-sum rule, e.g. by integrating the in-plane conductivity up to 1.5 eV, the result is approximately 4 eV [28], which is now in good agreement with the bare plasma frequency obtained from the LDA/RPA calculation. Hence we conclude that, although the f-sum rule provides us with in-plane and out-of-plane bare plasma frequencies reasonably close to estimates based on a simple band-structure approach, the plasma frequency and the frequency dependence of Re $\sigma(\nu)$ in both directions differ quantitatively and qualitatively from what is predicted by such a calculation.

The question of damping remains, but the discrepancy could be due to ignoring the strong correlation in high-T_c superconductors which is responsible for a metal-insulator transition at a relatively low doping level. Further theoretical considerations which address these issues will be given in Section 4.4.

4.2. *Conductivity and superfluid density*

Let E_g^* be the *effective* value of the gap, or gap distribution. We will assume $E_g^* = 3.5k_BT_c$, which becomes exact in the limit of a weak-coupling s-wave superconductivity. In the superconducting state we should make a distinction between the high- and low-frequency parts of the spectrum, i.e., far above and below E_g^* ($\approx$ 80 cm^{-1} for $La_{1.85}Sr_{0.15}CuO_4$). The former remains relatively unaffected by the superconducting transition, whereas for the latter range of frequencies we expect to find temperature dependence in both the real and imaginary parts of the electronic contribution to the conductivity. For example, for an isotropic s-wave BCS superconductor one expects a decrease of $\sigma(\nu)$ for $\nu \approx E_g^*/2$ as indicated in Fig. 8 (chained curve). In addition there may be strong decrease of γ for $T < T_c$ as has been reported for the in-plane infrared [29,30] and microwave [31] response of high-T_c superconductors, and for the c-axis infrared response of $La_{2-x}Sr_xCuO_4$ [7].

Also shown in Fig. 8 are the results of model calculations for the dirty limit of s-wave [32] and d-wave [33] superconductors, assuming standard ratios of E_g^*/T_c for these two models, and assuming a

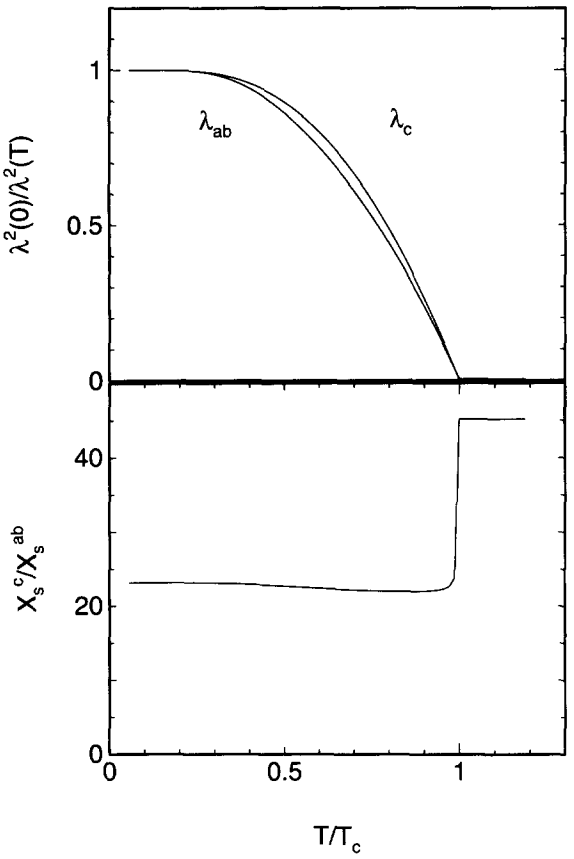

Fig. 8. The temperature dependence of $\tilde{\nu}_\phi^2$ (upper panel) and σ_n (lower panel) corresponding to the fits in Fig. 4. Squares: sample 1 with a constant $\tilde{\epsilon}_\infty$. Triangles: sample 2 with full frequency dependence of phonon oscillators included in $\tilde{\epsilon}_\infty$. Dashed curve: $1-(T/T_c)^4$. Chained curves: s-wave case simulations of superfluid fraction (upper panel) and the conductivity ratio (σ_s/σ_n) (lower panel). Solid curves: d-wave case simulations of superfluid fraction (upper panel) and the conductivity ratio (σ_s/σ_n) (lower panel). The simulations of the conductivity ratios are at $\nu = 50\ \mathrm{cm}^{-1}$.

temperature-independent scattering rate. The conductivity was calculated for $\nu = 50\ \mathrm{cm}^{-1}$. This frequency is close both to BCS gap energy $3.5k_BT_c = 80\ \mathrm{cm}^{-1}$ and to the gap value deduced from neutron scattering measurements [34]. As a result we observe for the s-wave model a steep drop of σ for $T < T_c$, and a kink at the temperature where $E_g(T) = h\nu$. If we would assume that in addition there is a drop of the scattering rate γ below T_c then the conductivity first increases, but, when γ reaches the gap energy, it decreases rapidly. Depending on the rate of decrease in γ this peak can be extremely narrow. Therefore when we assume a sudden reduction of γ below T_c, as done by Tamasaku et al., the theoretical conductivity curves would have an even steeper temperature dependence with a peak directly below T_c. For this reason we attribute the decrease of σ for $T < T_c$ exclusively to the opening of a gap, i.e., without, assuming a change of the electronic scattering rate. For d-wave pairing the calculated temperature dependence of the conductivity σ is smooth and is quite close to the experimentally determined values.

For $\sigma_n(T)$ a reasonable agreement exists with the d-wave model, whereas there is poor agreement with the s-wave model. For the normalized superfluid fraction $f_s(T) = (\tilde{\nu}_\phi(T)/\tilde{\nu}_\phi(0))^2$ the situation is reversed: f_s follows roughly the $1-(T/T_c)^4$ law, which differs strongly from the d-wave pairing curve, and lies somewhat above the s-wave pairing curve. The inconsistency with the d-wave curve can be removed if the strongly incoherent nature of the transport in the c direction is taken into account [35]. Recently Graf et al. [35] calculated the dynamical properties of a stack of two-dimensional d-wave superconductors along the c direction assuming that the hopping between planes occurs only due to scattering at impurity sites. The temperature dependence of f_s was found to be of the Ambegaokar-Baratoff type [36,37], *i.e.*, much closer to the experimental results.

For $\sigma_n(T)$ the comparison with the s-wave model can be improved if we postulate the existence of constant background (possibly spurious) conductivity in our samples. To the best of our knowledge, however, there is no experimental evidence to justify such a procedure.

Based on the clean-limit parameters of Ref. [7], Shibauchi et al. [12] could not explain their penetration depth data using a three-dimensional model. To illustrate how the anisotropy of $\sigma(\nu)$ influences that of the penetration depth, we calculated the ab-plane and the c-axis penetration depths, as well as the surface reactance assuming clean-limit parameters for the ab plane and dirty limit parameters for the c-axis. Since we do not expect the symmetry of the order parameter to be critical for the illustration of this particular point, we assumed s-wave pairing. The difference in behavior for both directions arises from the fact that in the dirty limit the c-axis penetration depth follows the Ambegaokar–Baratoff expression. As can be seen in Fig. 9, the jump in the anisotropy of the surface reac-

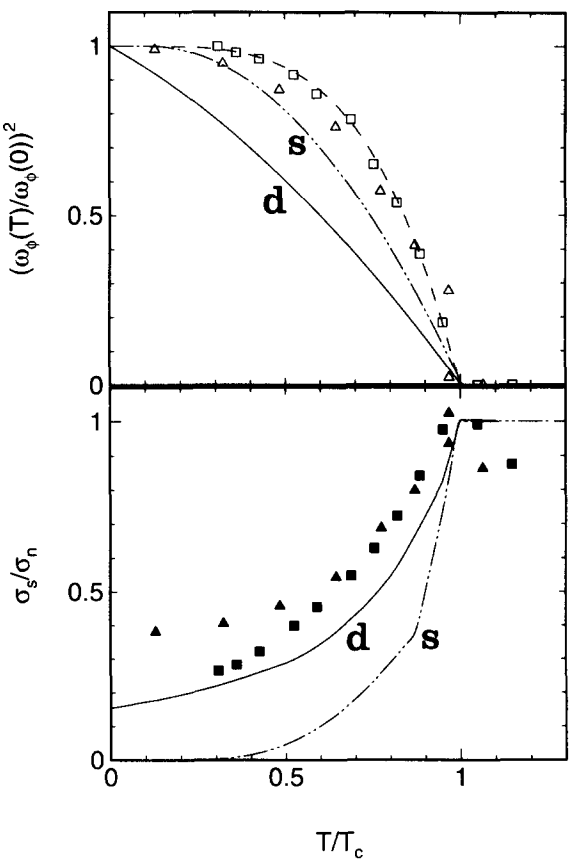

Fig. 9. Upper panel: the temperature dependence of $\lambda_{ab}^2(0)/\lambda_{ab}^2(T)$ and $\lambda_c^2(0)/\lambda_c^2(T)$ calculated using the BCS model. For $\boldsymbol{E} \parallel \boldsymbol{c}$ we used the Drude parameters $\epsilon_\infty = 25$, $\nu_p = 1200\ \mathrm{cm}^{-1}$, and $\gamma = 4500\ \mathrm{cm}^{-1}$. For $\boldsymbol{E} \perp \boldsymbol{c}$ we used $\epsilon_\infty = 5$, $\nu_p = 6000\ \mathrm{cm}^{-1}$, and $\gamma = 50\ \mathrm{cm}^{-1}$. Lower panel: the temperature dependence of the anisotropy of the surface reactance X_s^c/X_s^{ab}.

tance $X^c(T)/X^{ab}(T)$ [12] and the difference between λ_{ab} and λ_c follow naturally from our analysis with the anisotropy of $\sigma(\nu)$ properly taken into account.

4.3. Classification of infrared response of superconductors

In Fig. 10 we classify various regimes that can occur depending on the relevant energy scales. First, there is the pair-breaking energy scale E_g^*. Second is the screened plasma frequency $\tilde{\nu}_p = \tilde{\epsilon}_\infty^{-1/2}\nu_p$, ($\tilde{\epsilon}_\infty$ may include optical phonons depending on how far down the plasmon is pushed due to screening and damping

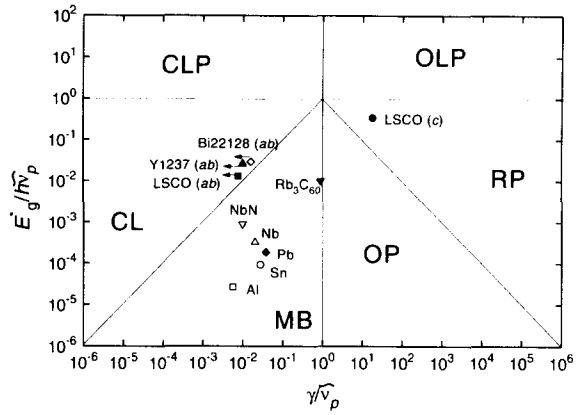

Fig. 10. The phase diagram in the $(\gamma/\tilde{\nu}_p)$-$(E_g^*/h\tilde{\nu}_p)$ plane. CL for 'clean limit,' MB for 'Mattis-Bardeen,' OP for 'Overdamped Plasmon,' RP for 'Re-entrant Phason,' CLP for 'clean local pair,' and OLP for 'overdamped local pair.'

effects). Similar parameters were also used by Uemura et al. [38] to classify clean-limit superconductors corresponding to their Fermi energy ($\propto h\nu_p$ for a two-dimensional Fermi liquid). We extend this classification with the scattering rate γ (using $2\gamma\sigma_0 = \nu_p^2$). We scale both E_g^* and γ to $\tilde{\nu}_p$.

The region labeled 'CL' corresponds to the clean limit where $\gamma \ll E_g^*$, and this region contains the 'exotic' superconductors considered by Uemura et al. [38], in particular the high-T_c cuprate superconductors characterized by their in-plane electrodynamical properties. Most classical superconductors fall in the region labeled 'MB,' where the infrared properties can be described in the context of dirty-limit Mattis-Bardeen theory. In the CL and MB regions a plasmon is found well above E_g^* in the normal as well as in the superconducting state.

In the regions labeled 'OP' and 'RP,' the plasmon is overdamped in the normal state, as with $\gamma > \tilde{\nu}_p$ a zero crossing of ϵ' no longer exists. In the superconducting state the 'missing area' of the conductivity due to the opening of the gap is transferred to the δ-function at $\nu = 0$, so that ϵ' crosses zero at $\tilde{\nu}_\phi = \tilde{\nu}_p\sqrt{\pi E_g^*/2h\gamma}$. Unless this frequency is below the gap, the plasma mode will be damped (OP region). Hence the requirement for the existence of a long-lived collective mode is that $E_g^*/\tilde{\nu}_p > \pi\tilde{\nu}_p/2\gamma$ (RP region). Using Anderson's expressions [39] for collective modes in the superconducting state it was recently shown [40], that the plasmon gradually changes from a collective oscil-

lation of quasi-particles for $\nu \gg E_g^*$ to an oscillating current carried by the condensate for $\nu \ll E_g^*$.

Our investigation indicates that the c-axis response of $La_{1.85}Sr_{0.15}CuO_4$ lies in this RP region. Although the c-axis response data for other high-T_c materials are very limited, the far-infrared results of Noh et al. [41] and of Tajima et al. [8] indicate that the c-axis response of $Nd_{1.85}Ce_{0.15}CuO_{4-y}$ and of $Bi_2Sr_2CaCu_2O_{8+x}$ should also be placed in the RP region. In both of these materials the c-axis plasmon, attributed to a sphere resonance by Noh et al. [41], is found at very low energy of approximately 10 cm^{-1}. In $Bi_2Sr_2CaCu_2O_{8+x}$ [8] and in $YBa_2Cu_3O_{7-\delta}$ [42], a very strong damping of the c-axis electronic response is observed.

The two regions labeled 'CLP' and 'OLP' correspond to clean- and dirty-limit superconductors with a pair-breaking energy larger than the plasma frequency. In such systems the phase transition is induced by thermal activation of phasons, while the pairs remain intact up to a higher de-pairing temperature scale. This corresponds to Bose-Einstein condensation of local pairs. According to the analysis of Tamasaku et al. [7] the c-axis phason of $La_{2-x}Sr_xCuO_4$ would be located in the CLP region.

4.4. Microscopic considerations

Here we give some theoretical considerations as to the origin of the strong damping along the c-axis, which is responsible for the absence of the c-axis plasma edge in the normal state and for the reduction of the c-axis plasma frequency in the superconducting state. In the case of $La_{1.85}Sr_{0.15}CuO_4$, one can argue that the replacement of La^{3+} ions with Sr^{2+} ions in 15% of the unit cells provides the necessary disorder. In principle it is possible to construct a potential landscape that is largely translation-invariant along the planes with the translational symmetry broken in the c direction, which leads to states localized in the c direction while remaining itinerant in the planar direction. Such a construction does not arise in a natural way from random substitution of La with Sr. Moreover the absence of a c-axis plasma edge above T_c and the reduction of the c-axis plasma frequency are also observed in fully doped $YBa_2Cu_3O_7$ [42] in which the Cu–O chains are presumably well ordered and the c-axis transport data shows T-linear temperature dependence of resistivity. Hence a broad and featureless $\sigma(\nu)$ in the c direction appears to be a *generic feature* of the high-T_c cuprate superconductors, which implies that this is a fundamental property of these materials.

Also our observation shows no signature of a large mass renormalization, which seems to contradict the notion of strongly renormalized Fermi-liquid behavior. On the other hand, the featureless line-shape of $\sigma(\nu)$ up to at least 0.5 eV demonstrates that there is no energy scale below which Fermi-liquid behavior sets in.

The aforementioned experimental observations can be explained within the framework of the theory of superconductivity based on the interlayer tunneling mechanism [43,16,44] by Anderson and co-workers. In this theory the single-particle tunneling between the planes is suppressed due to the formation of a Luttinger liquid state. As a result the dominant transport mechanism in the superconducting state is a Josephson-type pair-tunneling matrix element. Our observation that the dynamical conductivity at frequencies larger than the pair breaking energy of order $4k_BT_c$ remains basically unaffected by the superconducting phase transition, must then imply that the transition to the superconducting state only affects the dynamical properties of ground-state up to an energy scale of order $4k_BT_c$. The implication seems to be, that if the normal state is a Luttinger liquid, in the superconducting state dynamical properties of Fermi-liquid type are only restored up to frequencies of about $4k_BT_c$.

5. Conclusion

We conclude that the absence of a c-axis plasmon in the normal state of high-T_c cuprate superconductors results from an anomalously strong damping of the transport perpendicular to the CuO_2 planes. This assignment also alleviates the discrepancy by two orders of magnitude existing in the literature, between the plasma frequency obtained from optical experiments and that from the single-electron interlayer-hopping matrix element. The appearance of a c-axis phason mode, as observed in the superconducting state, is also a direct consequence of the anomalously strong damping of the charge-carrier transport perpendicular to the planes. The decrease in the c-axis conductivity

for $T < T_c$ can be fully accounted for by the opening of a gap, the presence of which is a necessary consequence of the f-sum rule. There is no indication for sudden decrease of the optical scattering rate for $E//c$ when $T < T_c$.

Acknowledgements

We gratefully acknowledge stimulating discussions with P. W. Anderson during the preparation of this manuscript. This investigation was supported by the Netherlands Foundation for Fundamental Research on Matter (FOM) with financial aid from the Nederlandse Organisatie voor Wetenschappelijk Onderzoek (NWO).

Note added in proof

After this paper was completed a preprint by Prokrovsky and Prokrovsky [45] came to our attention, where they carry out a theoretical analysis of the c-axis dynamical properties which is similar in philosophy to our work.

References

[1] U. Walter, M.S. Sherwin, A. Stacy, P.L. Richards and A. Zettl, Phys. Rev. B 35 (1987) 5327.
[2] P.E. Sulewski, A.J. Sievers, S.E. Russek, H.D. Hallen, D.K. Lathrop and R.A. Buhrman, Phys. Rev. B 35 (1987) 5330.
[3] Z. Schlesinger, R.L. Greene, J.G. Bednorz and K.A. Müller, Phys. Rev. B 35 (1987) 5334.
[4] D.A. Bonn, J.E. Greedan, C.V. Stager, T.Timusk, M. G. Doss, S.L. Herr, K. Kamarás, C.D. Porter, D.B. Tanner, J.M. Tarascon, W.R. McKinnon and L.H. Greene, Phys. Rev. B 35 (1987) 8843.
[5] Z. Schlesinger, R.T. Collins, M.W. Shafer and E.M. Engler, Phys. Rev. B 36 (1987) 5275.
[6] M.S. Sherwin, P.L. Richards and A. Zettl, Phys. Rev. B 37 (1988) 1587.
[7] K. Tamasaku, Y. Nakamura and S. Uchida, Phys. Rev. Lett. 69 (1992) 1455.
[8] S. Tajima, G.D. Gu, S. Miyamoto, A. Odagawa and N. Koshizuka, Phys. Rev. B 48 (1993) 16164.
[9] M. Bauer, Ph.D. Thesis, University of Tübingen, 1990.
[10] C.C. Homes, T. Timusk, R. Liang, D.A. Bonn and W.N. Hardy, Phys. Rev. Lett. 71 (1993) 1645.
[11] D.N. Basov, T. Timusk, B. Dabrowski and J.D. Jorgensen, Phys. Rev. B 50 (1994) 3511.
[12] T. Shibauchi, H. Kitano, K. Uchinokura, A. Maeda, T. Kimura and K. Kishio, Phys. Rev. Lett 72 (1994) 2263.
[13] P.W. Anderson, Science 235 (1987) 1196.
[14] F.C. Zhang and T.M. Rice, Phys. Rev. B 37 (1988) 3759.
[15] M.J. Rice and Y.R. Wang, Phys. Rev. B 48 (1993) 12921.
[16] D.G. Clarke, S.P. Strong and P.W. Anderson, Phys. Rev. Lett. 72 (1994) 3218.
[17] S. Chakravarty and P.W. Anderson, Phys. Rev. Lett. 72 (1994) 3859.
[18] M.J. Graf, D. Rainer and J.A. Sauls, Phys. Rev. B 47 (1993) 12098.
[19] A.G. Rojo and K. Levin, Phys. Rev. B 48 (1993) 16861.
[20] K. Levin, private communication. $\tilde{t}_\perp$ is smaller than the bare interlayer hopping energy $t_\perp$ by a factor of $\sim$4 due to many-body effects.
[21] V.H.M. Duijn et al., to be published.
[22] D. van der Marel, M. Bauer, E.H. Brandt, H.-U. Habermeier, D. Heitmann, W. König and A. Wittlin, Phys. Rev. B 43 (1991) 8606.
[23] S. Doniach and M. Inui, Phys. Rev. B 41 (1990) 6668.
[24] M. Czyzyk, unpublished.
[25] A. Fetter, Ann. Phys. 81 (1973) 367.
[26] A. Fetter, Ann. Phys. 88 (1974) 1.
[27] J.H. Kim, I. Bozovic, J.S. Harris Jr., W.Y. Lee, C.-B. Eom, T.H. Geballe, and E.S. Hellman, Physica C 185–189 (1991) 1019.
[28] This one can calculate easily by considering the phenomenological result that $\gamma(\nu)$ in the generalized Drude formula describing the in-plane conductivity is proportional to ν between 100 cm^{-1} and 10000 cm^{-1}. Taking these values as the lower and upper limits of the integration, and assuming a background dielectric constant $\epsilon_\infty = 4$, one obtains from the f-sum rule that the bare ν_p is about 4 times the frequency where $\epsilon' = 0$.
[29] D.B. Romero, C.D. Porter, D.B. Tanner, L. Forro, D. Mandrus, L. Mihaly, G.L. Carr and G.P. Williams, Phys. Rev. Lett. 68 (1992) 1590.
[30] M.C. Nuss, P.M. Mankiewich, M.L. O'Malley, E.H. Westerwick and P.B. Littlewood, Phys. Rev. Lett. 66 (1991) 3305.
[31] D.A. Bonn, R. Liang, T.M. Riseman, D.J. Baar, D.C. Morgan, K. Zhang, P. Dosanjh, T.L. Duty, A. MacFarlane, G.D. Morris and Brewer, Phys. Rev. B 47 (1993) 11314.
[32] D.C. Mattis and J. Bardeen, Phys. Rev. 117 (1958) 912.
[33] H. Won and K. Maki, Phys. Rev. B 49 (1994) 1397.
[34] T.E. Mason, G. Aeppli and H.A. Mook, Phys. Rev. Lett. 68 (1993) 1414.
[35] M.J. Graf, unpublished.
[36] V. Ambegaokar and A. Baratoff, Phys. Rev. Lett. 10 (1963) 486.
[37] V. Ambegaokar and A. Baratoff, Phys. Rev. Lett. 11 (1963) 104.
[38] Y.J. Uemura, L.P. Le, G.M. Luke, B.J. Sternlieb, W.D. Wu, J.H. Brewer, T.M. Riseman, C.L. Seaman, M.B. Maple, M. Ishikawa, D.G. Hinks and J. Jorgensen, Phys. Rev. Lett. 66 (1991) 2665.
[39] P.W. Anderson, Phys. Rev. 112 (1958) 1900.

[40] D. van der Marel, Phys. Rev. B 51 (1995) 1147.
[41] T.W. Noh, S.G. Kaplan and A.J. Sievers, Phys. Rev. B 41 (1990) 307.
[42] J. Schützmann, S. Tajima, S. Miyamoto and S. Tanaka, Phys. Rev. Lett. 73 (1994) 174.
[43] S. Chakravarty, A. Sudbø, P.W. Anderson and S. Strong, Nature 261 (1993) 337.
[44] P.W. Anderson, Science, in press (1995).
[45] S.V. Prokrovsky and V.L. Prokrovsky, preprint.